



Experimental investigation of temporal evaluations of scouring downstream of culvert

Soroush Jafari¹ · Mohammad Vaghefi² · Amin Mahmoudi²

Received: 12 January 2023 / Accepted: 16 April 2024 / Published online: 13 May 2024
© The Author(s) 2024

Abstract

The investigation of bed topography downstream of culverts is very important. Since bed topography goes through extreme changes through time, this study investigated the temporal evaluations of bed topography. Also, the bed level downstream of culverts, as one of effective parameters in topography in different time spans, was investigated. One of the most important findings of the study is that with increasing the experiment time and approaching the equilibrium moment, the change percentage of the maximum scour depth decreased. Also with changes to and decrease in the bed level downstream of the culvert, the change percentage of the depth scour decreased. Another salient finding of this study was that the maximum scour over the beginning durations of the tests in case of equal downstream level and culvert bed level was approximately equal to the maximum scour in cases where the downstream bed level differed from the culvert bed level by 0.067 and 0.13 times the culvert mouth width.

Keywords Culvert · Sedimentation · Bed topography · Bed level · Temporal evaluations · Equilibrium time

Introduction

Investigation of phenomena related to hydraulic structures such as scouring is an effective factor in the stability of hydraulic structures. Scouring occurs when bed materials are moved to another place by a transferring agent. There are numerous parameters that can bring about significant changes downstream of hydraulic structures. One of the parameters which can be investigated is the effect of temporal evaluations of bed topography downstream of hydraulic structures. Many researches have been done on the effect of time on bed topography downstream of hydraulic structure. Some of these studies will be introduced below.

Yanmaz and Altinbilek (1991), Melville and Chiew (1999), Mia and Nago (2003), Oliveto and Hager (2005), and Sung-uk Choi and Byungwoong (2016) investigated time-dependent local scouring around bridge piers (Yanmaz and Altinbilek 1991; Melville and Chiew 1999; Mia and Nago 2003; Oliveto and Hager 2005; Sung-Uk and Byungwoong 2016). Yanmaz and Kose (2007) and Ben Mohammad Khaje and Vaghefi (2020) investigated temporal evaluations of scouring in bridge abutments (Yanmaz and Kose 2007; Ben Mohammad Khajeh and Vaghefi 2020). Dodaro et al. (2014) carried out experimental and numerical studies of the changes to the place and time of formation of scour holes downstream of a solid bed (Dodaro et al. 2014). Aminpour et al. (2018) and Aksoy and Dogan (2019) investigated time-dependent local scouring downstream of a spillway (Aminpour et al. 2018; Aksoy and Dogan 2019). Eghbalnik et al. (2019) carried out an experimental study of temporal evaluations of bed topography in presence of two rows of inclined-vertical piers in a 180-degree sharp bend (Eghbalnik et al. 2019). Safaripour et al. (2020) studied the effects of the submergence ratio of the double-submerged vanes located upstream of a pier group on the topographic changes and the timing of the maximum scour in a 180-degree sharp bend (Safaripour et al. 2020). Solati and Vaghefi (2020) investigated the effect of the duration and hydrograph pattern of scouring around

✉ Mohammad Vaghefi
Vaghefi@pgu.ac.ir

Soroush Jafari
Soroushgj@yahoo.com

Amin Mahmoudi
A_mahmoudi@pgu.ac.ir

¹ Department of Civil Engineering, Persian Gulf University, Bushehr, Iran

² Department of Civil Engineering, Faculty of Civil Engineering, Persian Gulf University, Bushehr, Iran

piers in a sharp bend under incipient motion and living bed (Solati and Vaghefi 2020). Vaghefi et al. (2009) and Pandey et al. (2021) experimentally evaluated and predicted the scour depth around spur dikes (Vaghefi et al. 2009; Pandey et al. 2021). Moghaddassi et al. (2021) investigated the effect of time on bed topography in a meandering channel (Moghaddassi et al. 2021). In this paper, the performance of a culvert and the effect of temporal evaluations and bed level variations on bed topography downstream of the culvert are investigated.

So far, many researchers have investigated scouring downstream of culverts, some of which are given below. Abt et al. (1985) studied how the slope of a culvert affects the depth, length, width and volume of scour holes. Experiments were done involving culverts with 0, 2, 5, 7 and 10 percent slopes. The results showed that the scour depth increased with the increase in the slope of the culvert (Abt et al. 1985). Abt et al. (1987) investigated the different shapes of culverts, including arc, square, rectangular and circle shapes. They expressed the relative length of the scour hole for different

Fig. 1 Experimental setup

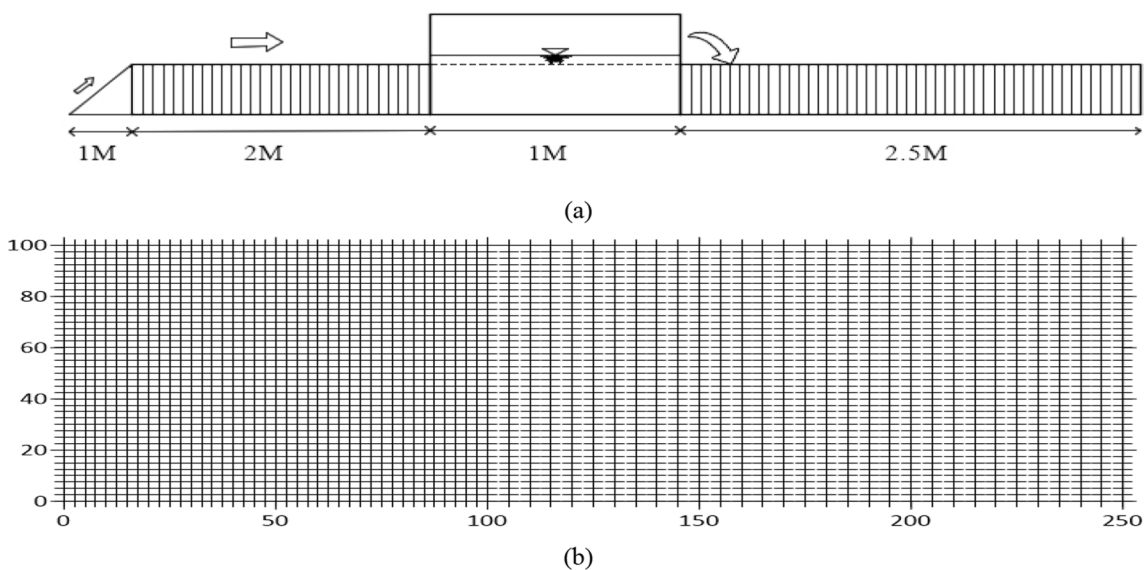


Fig. 2 Schematic of a channel side view b meshing plan

culvert shapes as a function of flow intensity. The scouring length of square and rectangular culverts were almost the same. These values were 10–30 percent higher than those of the circular culvert (Abt et al. 1987). Doehring and Abt (1994) investigated the drop height of the water jet coming out of a culvert on the dimensions of the local scour. It was found that the culverts located at the levels above the bed created deeper and wider holes than those located near the bed (Doehring and Abt 1994). Emami and Shciels (2010) carried out experiments in live-bed conditions in order to compare local scouring in different situations. The results showed that, for the low and high tailwater depths, the maximum scouring depths were respectively about 30% and 40% of the maximum scouring length of the culvert outlet. Also, the length of the scour hole increased while the width of the hole decreased with increase in the tailwater level (Emami and Shciels 2010). Sorourian et al. (2013) conducted an experimental study of scour at the outlet of a non-blocked and a partially blocked culvert under unsteady flow conditions and investigated the relative effect of blocking on the scour pattern. They found that 88–98% of the maximum scour depth occurred in the ascending branch of the hydrograph (Sorourian et al. 2013). Zhang and Peng (2019) investigated the maximum scour depth in the outlet

of a rectangular and a circular culvert and compared the results with those of the previous articles. They noticed that the prediction of the Abt equation for circular culverts was about 85% (Zhang and Peng 2019). Horst (2019) investigated the effect of several side walls with different angles. The results showed that, by changing the angle of the wall, the amount of scouring changed and the highest scouring depths occurred when there was no wall or the side wall was short and diagonal, and the lowest scouring depth was associated with long walls (Horst 2019). Galan et al. (2019) showed that the shape of the culvert affected the length and width of the scour hole and the effect of the square culvert on the length of the scour hole was greater than that of the circular culvert. They also argued that by increasing the tailwater depth, the scour hole become shallower (Galan and Gonzalez 2019). Gunal et al. (2019) compared the simulated Flow 3D results of a box culvert with Sorourian’s experimental results to evaluate the accuracy of the numerical model (Gunal et al. 2019). Nasreen et al. (2020a) conducted numerical and experimental investigations of scour depths downstream of a culvert in different blockage conditions. They used Flow-3D for numerical analysis. Four blockage conditions of the culvert height were investigated: 0, 30, 50, and 70 percent (Nasreen et al. 2020a). Nasreen et al. (2020b)

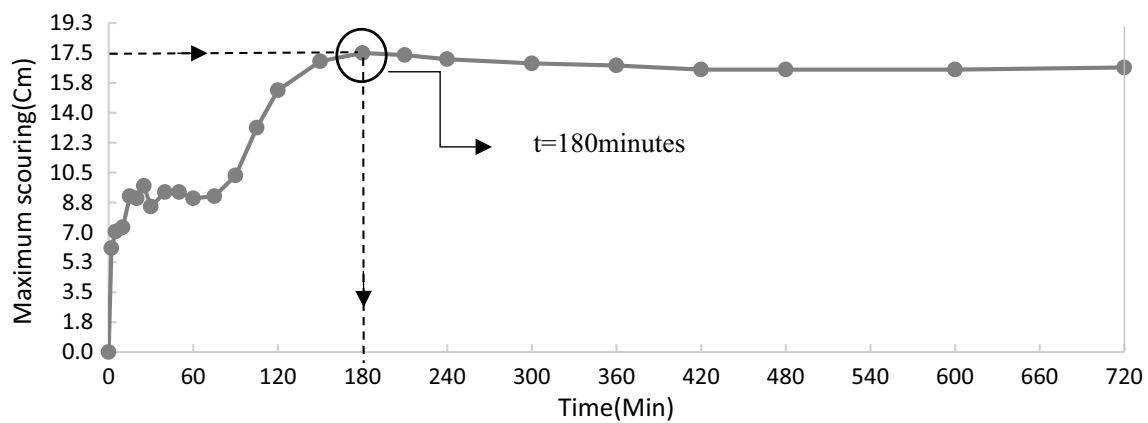


Fig. 3 Maximum scour depth variations during the equilibrium time

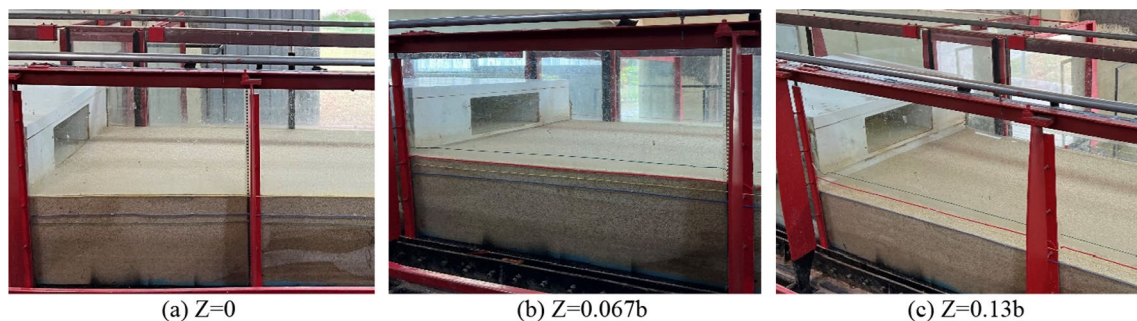
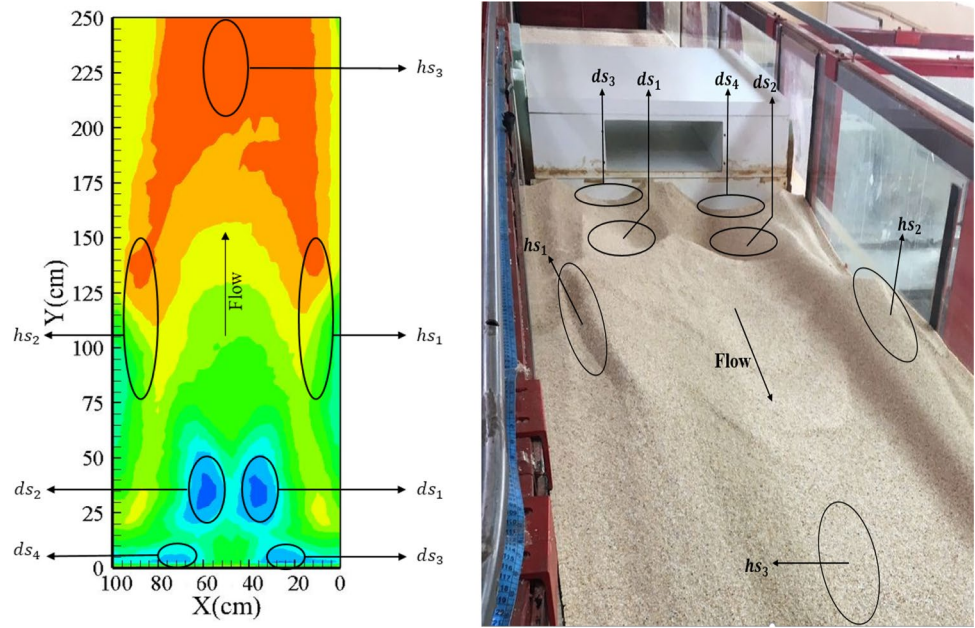


Fig. 4 Different bed levels downstream of culvert

Fig. 5 Illustrates the schematic and real zone of significant points downstream of the culvert



stated that the accumulation of sediments in the upstream and through the passage of hydraulic structures such as culverts caused the water level to increase and the downstream scour depth to increase, which could lead to the failure of the structure. The results showed that by increasing the absorption ratio, the maximum scour depth decreased at the same flow rate. Also, by increasing the Froude number, the scouring depth increased (Nasreen et al. 2020b). Ahmed et al. (2021) investigated the execution of numerical models in forecast scour depth and its location downstream of the culverts in unsteady flow situations. Culverts with unblocked

and semi-blocked ducts were used. The results showed that the numerical model had good agreement with the experimental data (Ahmed et al. 2021).

Sadeghpour et al. (2023) explored the effect of artificial roughness arrangement installed inside the culvert with different roughness dimensions on the bed scour pattern downstream of the culvert. They investigated the effect of obstacles against the flow which acted as dissipaters of flow energy and they presented the most efficient arrangement for artificial roughness in terms of creating the least

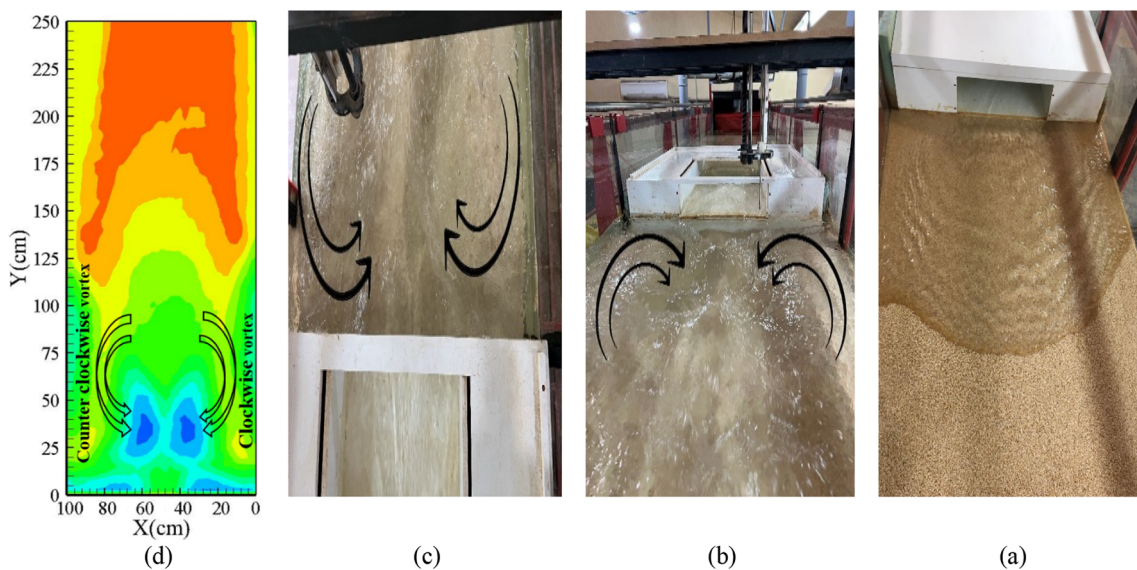


Fig. 6 Shows the output flow of the culvert at the zero level with a vortex downstream of the culvert

scour downstream of the culvert in case of downstream bed level with the culvert bed (Sadeghpour et al. 2023).

This study investigated bed topography variations at different time intervals from the test onset until the equilibrium time. Furthermore, to determine the effect of bed drop downstream of the culvert on bed topography variations, numerous tests were conducted for different

durations at varied levels (level with the culvert bed and 0.067 and 0.13 times the mouth width lower than the culvert bed). In addition, this study addressed the effect of temporal variations on the important points mentioned in the article in terms of scouring and sedimentation, such as the maximum scour depth, the maximum sedimentation height, the fourfold slopes of the scour hole as well

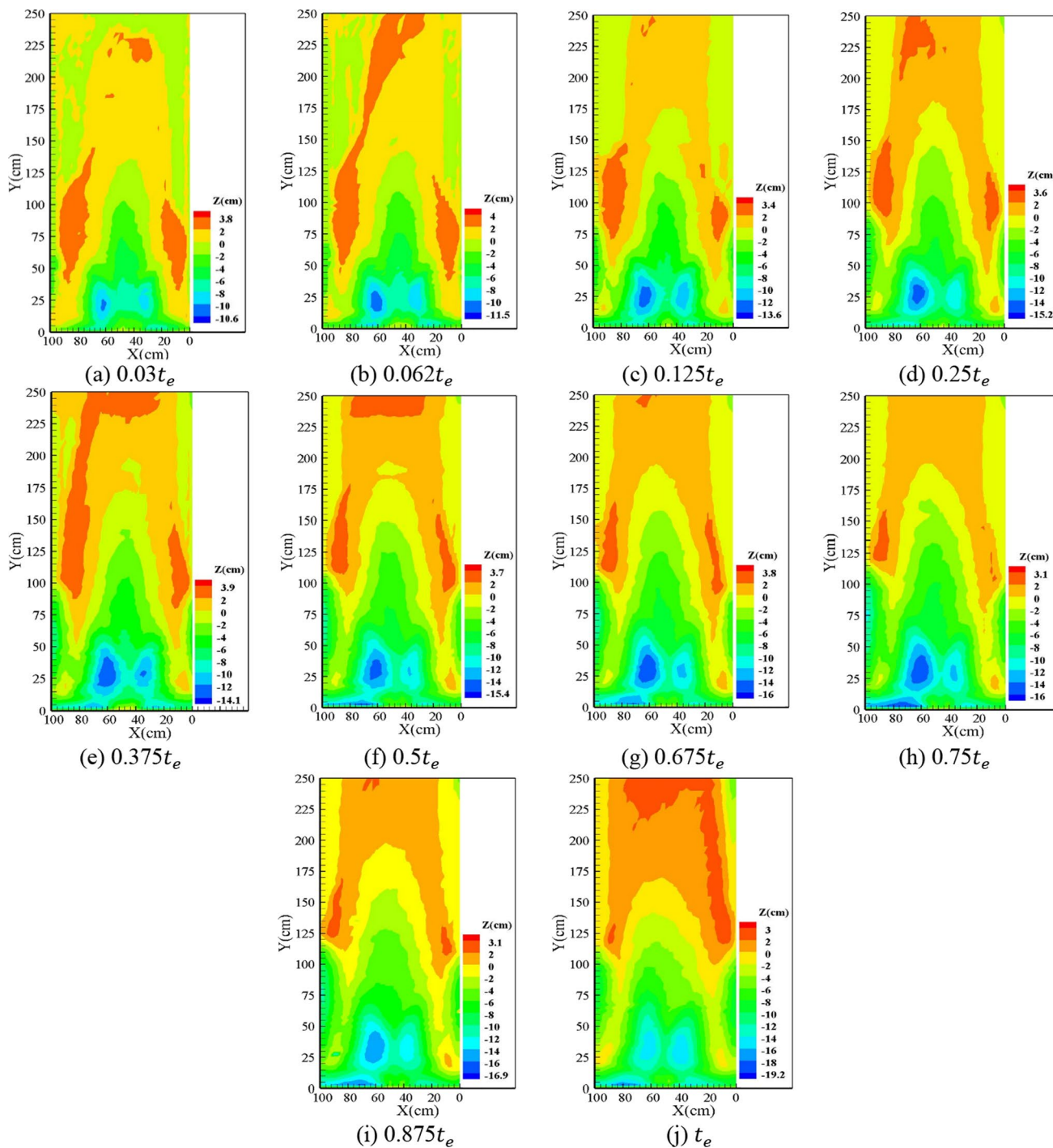


Fig. 7 Bed topography changes downstream of culvert at level $Z=0$

as the volume and area of the scour holes. Instances of the transverse and longitudinal profiles on important bed axes were also discussed.

Materials and methods

The culvert used in this study was located in a straight path which was 6.5 m long and 1 m wide and in a rectangular flume. The culvert was located 3 m away from the flume inlet. The length and width of the culvert were assumed to be 1 m and 0.45 m, respectively. Figure 1 shows the culvert's location in the flume with its dimensions.

Before conducting the experiments, the bed levels downstream and upstream of the culvert was leveled with a bed smoothing device. According to Fig. 2a, the flow entered from the straight path upstream of the culvert and flowed out downstream of the culvert. In all experiments, the discharge capacity was $0.0215 \text{ m}^3/\text{s}$. At the end of the experiment, when the water in the channel was drained, the bed topography was obtained with a laser device. A $0.025 \text{ m} \times 0.025 \text{ m}$ mesh grid was used over the first 1 m and a $0.05 \text{ m} \times 0.025 \text{ m}$ mesh grid was utilized over the next 1.5 m downstream of the culvert in the straight path. For this purpose, 70 longitudinal sections and 40 transvers sections were obtained. Figure 2b illustrates the meshing downstream of the culvert.

Figure 3 illustrates the equilibrium time experiment, which lasted for 720 min. As shown in the figure, the scour depth reached the maximum amount at minute 180, and, after that, with continuous crumbling of the wall into the hole over time, the maximum scour depth decreased. Therefore, 180 min was considered as the equilibrium time (t_e) in all experiments.

Nine other experiments with 0.03, 0.062, 0.125, 0.25, 0.375, 0.5, 0.625, 0.75, and 0.875 of the equilibrium time were conducted. All experiments were conducted at 3 different bed levels which had been made dimensionless with respect to the width of the culvert (b). The bed

levels downstream of the culvert were $Z=0$, $Z=0.067b$ and $Z=0.13b$. The downstream bed levels of the culvert are shown in Fig. 4. The zero bed level was the level at which the height of the sediment was equal to that of the culvert outlet. The other two bed levels were those at which the height of the bed sediment was lower than that of the culvert outlet at the specified values.

In Fig. 5, the location of the zone of the significant points of scouring and sedimentation downstream of the culvert is shown.

In this figure, two scour holes are formed parallel to the culvert walls outlet at a distance of $0.08\text{--}0.2Y$ from the culvert, where Y is the length of the straight path downstream of the culvert. The maximum depth of the right and left scour holes are represented by ds_1 and ds_2 , respectively. In most experiments, maximum scouring occurred in this zone.

Also, some holes were formed in the vicinity of the culvert in the $0\text{--}0.02Y$ zone. In some experiments, maximum scour depth occurred within the holes. The maximum depths of right and left scour holes are indicated by ds_3 and ds_4 , respectively. Also, in different experiments, maximum sedimentation occurred in three different zones. Two sediment peaks formed near the banks and one peak in the middle of the channel. Maximum sedimentation on the right and left sides are indicated by hs_1 and hs_2 , respectively. These points of sedimentation were located in the range of $0.3\text{--}0.6Y$ from the culvert and at $0\text{--}0.2X$ from the right and left banks. hs_3 indicates the middle sedimentation peak. This peak was formed at $0.8Y\text{--}Y$ from the culvert and in $0.4\text{--}0.6X$ from the right bank.

The scour holes are located in one of the four regions of ds_1 , ds_2 , ds_3 and ds_4 depending on the parameters of the test time and the downstream bed topography level variations. Such changes in the location of the maximum scour depth in different tests are due to instability of the scour hole as a result of change in the falling jet impact (given the level change) as well as the development of the test time (considering the study of the temporal variations).

Fig. 8 Culvert output jet at level $Z=0.067b$



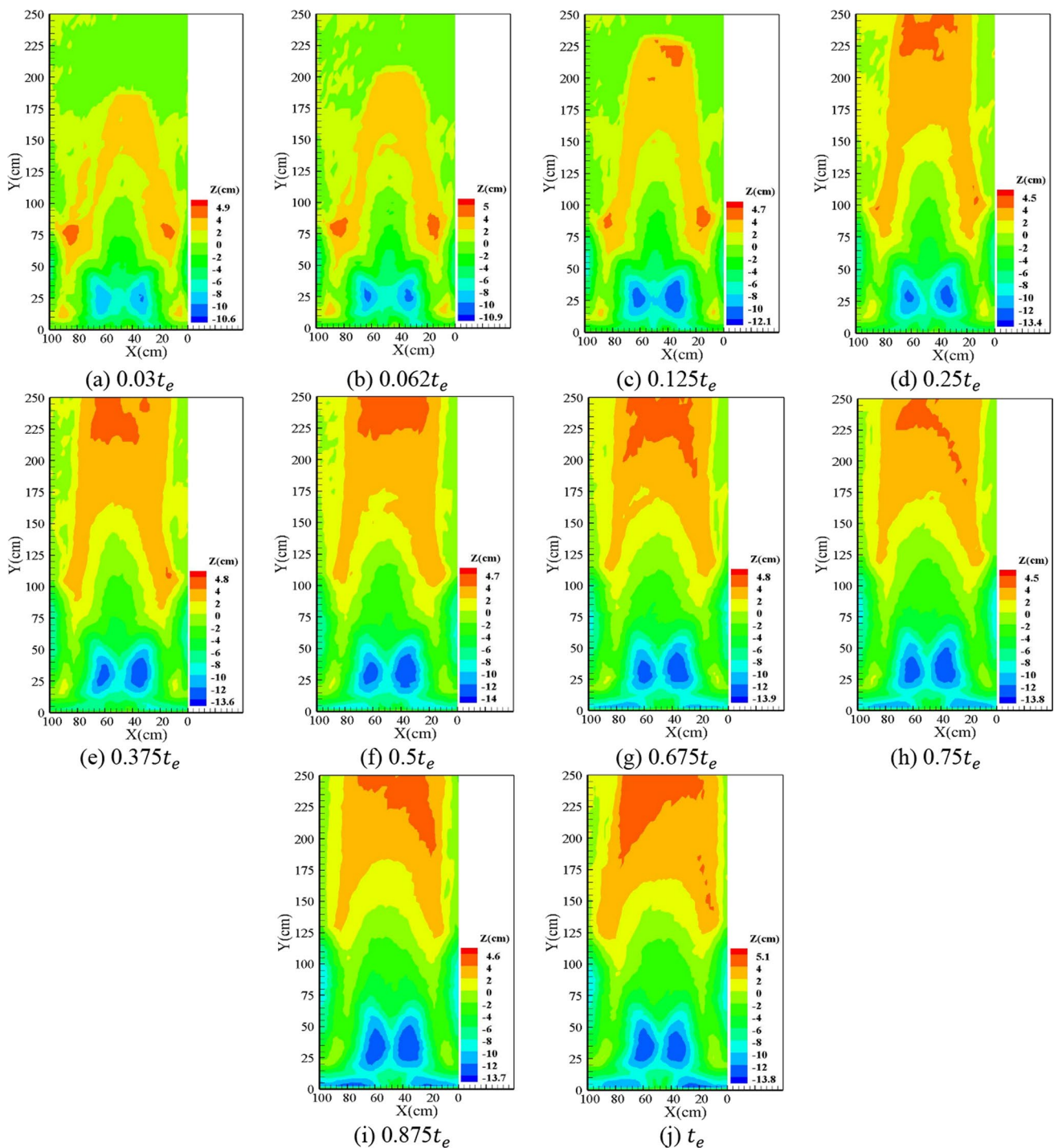


Fig. 9 Bed topography changes downstream of culvert at level $Z=0.067b$

Results and discussion

At zero bed level, the flow, after leaving the culvert, moved on the bed material. In the initial seconds, the flow coming out of the culvert created a score hole near the culvert. Then, the sediments were transferred to the downstream

of that hole. Figure 6a demonstrates how the flow came out of the culvert and hit the bed material. After about a minute, the scour hole which formed downstream of the culvert changed into two scour holes that were aligned with the external walls of the culvert. Some vortices were formed around the scour holes, as seen in Fig. 6b, c. These

Fig. 10 The water jet flowing out of the culvert at level $Z=0.13$



vortexes were formed clockwise near the right bank and counter-clockwise near the left bank. They transferred the bed material from the vicinity of the banks into the scour holes. Sedimentation occurred in the vortex zone, where the flow velocity was low. Figure 6d shows that sediment zones hs_1 and hs_2 were formed in the vortex zones.

Figure 7 represents the bed topography downstream of the culvert at $Z=0$ in different experiment time periods. As this figure shows, two scour holes were formed downstream of the culvert in all experiments. Also, as seen in the figure, in 90% of the experiments, the scour depth in ds_2 was greater than in ds_1 , and just in the equilibrium time experiment, the two holes reached balance. At this level, in all experiments, the area of ds_2 was larger than that of ds_1 . Also, with increasing the experiment time and approaching the equilibrium experiment, the areas of the two holes expanded. At this level, the maximum scour depth increased with increase in the time of the experiment from $0.3t_e$ to $0.25t_e$. The maximum scour hole decreased and maximum sedimentation increased with increasing the experiment time from $0.25t_e$ to $0.375t_e$. The maximum sedimentation occurred in hs_2 in $0.375t_e$. The counterclockwise vortexes which transferred the bed materials into the scour hole of ds_2 transferred more sediment into the hole with increase in the amount of sedimentation and filled the hole near the left bank (ds_2). When the hole was filled with sediment by the counterclockwise vortexes, the maximum scour depth, which had been formed by $0.375t_e$ in ds_2 , was transferred to ds_4 .

In 80 per cent of the experiments, at this level, maximum sedimentation occurred in zones hs_1 and hs_2 . At this level, with increasing the time and approaching the equilibrium time, the progress of the sediment toward the downstream of the culvert increased, and maximum sedimentation occurred downstream at a greater distance from the culvert.

At level $Z=0.067b$, because of the reduction in the bed level, the output flow hit the bed material as a jet. Figure 8 presents the culvert output jet at this level.

At level $Z=0.067b$, the amount of maximum scouring at the beginning of the experiment ($0.03 t_e$) was equal to that of level $Z=0$, but with increasing time up to the equilibrium time, the amount of maximum scouring decreased with respect to that level. With decrease in the bed level, the

height of water inside the holes increased, which caused the water inside the holes to act like a damper and prevent the output water jet from directly hitting the bed material, leading to decrease in the maximum scour depth.

Figure 9 shows the bed topography downstream of the culvert at level $Z=0.067b$ at different times. In 80% of the experiments, at this level, maximum scour depth occurred in the zone of ds_1 , but, in experiments with $0.062 t_e$ and t_e , the maximum scour depth appeared in ds_2 . At this level, the area of scour holes increased by increasing the time of the experiment. As seen in the figure, maximum scour depth increased until $t=0.5t_e$, and after that, the scour holes reached relative stability. In 50% of the experiments, at this level, maximum sedimentation appeared in hs_3 , which was different from that of $Z=0$, where maximum sedimentation occurred in hs_1 and hs_2 . The reason for this difference is that, at the $Z=0.067b$ level, the water depth was higher than that of the $Z=0$ level and the surface vortexes were weaker than those of the zero level. Therefore, sedimentation at the end of the vortexes was less than that of the zero level and the sediment was transferred further downstream of the channel.

At level $Z=0.013b$, as with level $Z=0.067b$, the flow after flowing out of the culvert hit the bed material in the form of a jet and caused scour holes downstream of the culvert. At this level, due to the increase in the height of the jet, the maximum scouring depth at the beginning of the experiment increased, compared to the other two levels, which was consistent with Doehring and Abt (1994) research. With increasing the time experiment, the jet hit the walls of the hole and led to destruction of the wall as well as falling of the materials into the hole, which reduced the amount of scouring in the experiment with $0.062t_e$. Figure 10 shows how the jet flowed out of the culvert and hit the bed material at level $Z=0.13b$.

Figure 11 illustrates the bed topography downstream of culvert at level $Z=0.13b$. At this level, as at level $Z=0.067b$, in 80% of the experiments, maximum scour depth appeared near the right bank (ds_1). Also, as with other two levels, with increasing the experiment time and approaching the equilibrium time, the hole area increased at this level. Moreover, the forward movement of sediments downstream of the culvert was less than those of the other two levels. At

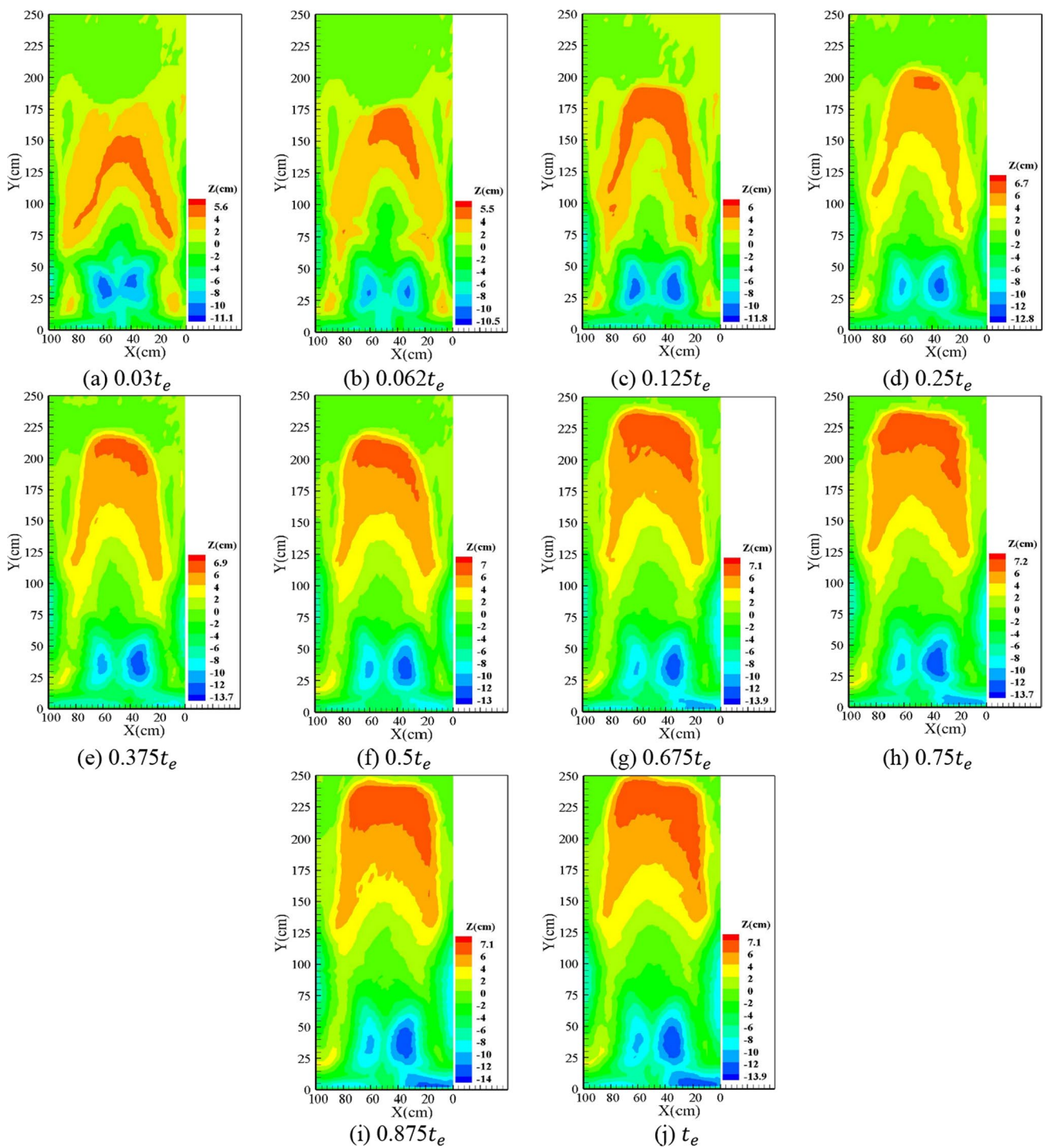


Fig. 11 Bed topography changes downstream of culvert at level $Z=0.13b$

level $Z=0.13b$, with decrease in the bed level, water depth in the channel increased, the flow did not hit the bed material directly, and water poured down into the water pond due to the initial difference between the surface of the bed and the culvert. Therefore, the erosion power of the stream

decreased and, as a result, the forward movement of the sediment downstream of the culvert decreased.

Due to the instability of the hole slopes, particularly at the beginning of each test and the fact that the slope angle of these holes were sharper than the particle' angle of repose during some time intervals, the hole wall fell into

Table 1 Percentages of reduction at levels $Z=0.067b$ and $Z=0.13b$ compared to $Z=0$

| Number | t/t_e | The percentage of the maximum reduction of depth of scouring at the level $Z=0.067b$ compared to the level $Z=0$ | The percentage of the maximum reduction of depth of scouring at the level $Z=0.13b$ compared to the level $Z=0$ |
|--------|---------|--|---|
| 1 | 0.03 | 0 | -4.7 |
| 2 | 0.062 | 5.5 | 9.5 |
| 3 | 0.125 | 12.4 | 15.2 |
| 4 | 0.25 | 13.4 | 18.7 |
| 5 | 0.375 | 3.6 | 2.9 |
| 6 | 0.5 | 10 | 18.4 |
| 7 | 0.625 | 15.1 | 15.1 |
| 8 | 0.75 | 15.9 | 16.7 |
| 9 | 0.875 | 23.3 | 20.7 |
| 10 | 1 | 39.1 | 38.1 |

Table 2 Maximum scour depth coordinates

| Number | t/t_e | $Z=0$ | | | $Z=0.067b$ | | | $Z=0.13b$ | | | | | |
|--------|---------|---------------------------------------|----------------------|---------------|---------------|---------------------------------------|----------------------|---------------|---------------|---------------------------------------|----------------------|---------------|---------------|
| | | The symbol for the location of points | $\frac{ds_{max}}{y}$ | $\frac{Y}{y}$ | $\frac{X}{y}$ | The symbol for the location of points | $\frac{ds_{max}}{y}$ | $\frac{Y}{y}$ | $\frac{X}{y}$ | The symbol for the location of points | $\frac{ds_{max}}{y}$ | $\frac{Y}{y}$ | $\frac{X}{y}$ |
| 1 | 0.03 | ds_2 | 1.18 | 3.70 | 11.57 | ds_1 | 1.18 | 5.21 | 6.77 | ds_2 | 1.23 | 7.29 | 12.50 |
| 2 | 0.062 | ds_2 | 1.28 | 4.17 | 11.57 | ds_2 | 1.21 | 5.73 | 13.02 | ds_1 | 1.67 | 6.77 | 6.77 |
| 3 | 0.125 | ds_2 | 1.51 | 4.63 | 11.57 | ds_1 | 1.34 | 5.73 | 7.29 | ds_1 | 1.31 | 7.29 | 6.77 |
| 4 | 0.25 | ds_2 | 1.69 | 5.10 | 11.57 | ds_1 | 1.49 | 6.25 | 7.29 | ds_1 | 1.42 | 7.29 | 7.29 |
| 5 | 0.375 | ds_2 | 1.57 | 5.10 | 11.11 | ds_1 | 1.51 | 6.77 | 7.29 | ds_1 | 1.52 | 7.29 | 7.29 |
| 6 | 0.5 | ds_4 | 1.71 | 0.46 | 12.96 | ds_1 | 1.56 | 6.77 | 7.29 | ds_1 | 1.44 | 7.29 | 6.77 |
| 7 | 0.625 | ds_2 | 1.78 | 5.10 | 11.11 | ds_1 | 1.54 | 7.29 | 7.81 | ds_1 | 1.54 | 7.81 | 7.29 |
| 8 | 0.75 | ds_4 | 1.78 | 0.46 | 12.96 | ds_1 | 1.53 | 7.81 | 7.81 | ds_1 | 1.52 | 7.29 | 7.81 |
| 9 | 0.875 | ds_4 | 1.88 | 0.46 | 12.96 | ds_1 | 1.52 | 7.81 | 7.29 | ds_3 | 1.56 | 0.52 | 2.60 |
| 10 | 1 | ds_4 | 2.13 | 0.46 | 14.81 | ds_2 | 1.53 | 7.81 | 11.98 | ds_1 | 1.54 | 7.29 | 7.29 |

Table 3 Maximum amounts of sedimentation and their locations

| Number | t/t_e | $Z=0$ | | | $Z=0.067b$ | | | $Z=0.13b$ | | | | | |
|--------|---------|---------------------------------------|----------------------|---------------|---------------|---------------------------------------|----------------------|---------------|---------------|---------------------------------------|----------------------|---------------|---------------|
| | | The symbol for the location of points | $\frac{hs_{max}}{y}$ | $\frac{Y}{y}$ | $\frac{X}{y}$ | The symbol for the location of points | $\frac{hs_{max}}{y}$ | $\frac{Y}{y}$ | $\frac{X}{y}$ | The symbol for the location of points | $\frac{hs_{max}}{y}$ | $\frac{Y}{y}$ | $\frac{X}{y}$ |
| 1 | 0.03 | — | 0.42 | 12.50 | 0.93 | hs_2 | 0.54 | 16.15 | 18.23 | — | 0.62 | 31.25 | 8.33 |
| 2 | 0.062 | hs_1 | 0.44 | 14.35 | 0.93 | hs_2 | 0.55 | 16.67 | 18.23 | — | 0.61 | 35.42 | 9.38 |
| 3 | 0.125 | hs_2 | 0.38 | 17.13 | 16.67 | hs_1 | 0.52 | 19.27 | 2.60 | — | 0.67 | 37.50 | 6.77 |
| 4 | 0.25 | hs_2 | 0.40 | 19.44 | 16.67 | hs_3 | 0.50 | 47.92 | 9.38 | hs_3 | 0.74 | 41.67 | 8.85 |
| 5 | 0.375 | hs_2 | 0.43 | 19.44 | 16.20 | hs_3 | 0.53 | 48.96 | 10.41 | — | 0.77 | 43.75 | 7.81 |
| 6 | 0.5 | hs_2 | 0.41 | 21.30 | 16.67 | hs_3 | 0.52 | 51.04 | 12.50 | hs_3 | 0.78 | 43.75 | 9.38 |
| 7 | 0.625 | hs_2 | 0.42 | 21.30 | 17.13 | — | 0.53 | 50 | 7.29 | hs_3 | 0.79 | 47.92 | 10.41 |
| 8 | 0.75 | hs_2 | 0.34 | 24.07 | 16.67 | hs_3 | 0.50 | 50 | 10.94 | hs_3 | 0.80 | 47.92 | 10.41 |
| 9 | 0.875 | hs_2 | 0.34 | 23.15 | 17.13 | — | 0.51 | 45.83 | 4.69 | hs_3 | 0.79 | 48.96 | 10.94 |
| 10 | 1 | hs_1 | 0.33 | 25.93 | 1.39 | hs_3 | 0.56 | 51.04 | 13.54 | hs_3 | 0.79 | 50 | 9.38 |

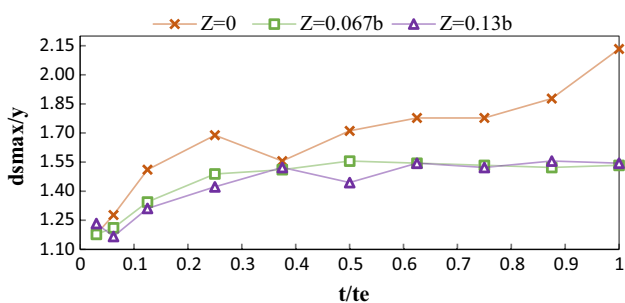


Fig. 12 Temporal evaluations of the maximum dimensionless scour depth at three different levels

the hole during the tests. This downfall varies depending on the conditions of each test in terms of the test duration and the downstream bed level. Therefore, over time and with changes in the topography of the holes, complete asymmetry occurs, particularly at the beginning, and lasts to the end of the tests. In fact, throughout the downstream bed topography, there is a relative symmetry but complete asymmetry.

According to Figs. 7, 9, 11, the maximum scour depth at level $Z=0$ and in the experiment with $0.125 t_e$ reached 98%

Table 4 Coefficients of the equations for predicting the maximum scour depth and sedimentation

| Bed level | ds_m/y | | hs_m/y | |
|--------------|----------|-------|----------|--------|
| | a | b | a | b |
| $Z=0.0b$ | 1.92 | 0.220 | 0.40 | 0.0125 |
| $Z = 0.067b$ | 1.59 | 0.122 | 0.54 | 0.087 |
| $Z = 0.13b$ | 1.54 | 0.051 | 0.75 | 0.10 |

of the maximum scour depth in the equilibrium time at levels $Z=0.067b$ and $Z=0.13b$.

Table 1 compares the decreases in the percentage of the scour depth at levels $Z=0.067b$ and $Z=0.13b$ with that of level $Z=0$ in each experiment time. As seen in the table, in all experiment time periods, expect for the initial time of $0.03 t_e$, the maximum scour values at levels $Z=0.13b$ and $Z=0.067b$ were less than that of level $Z=0$. The reason for the lack of reduction in scouring depth in this experiment time ($0.03 t_e$) was that the output jet hit the bed in the first minutes of the test. Also, according to Figs. 7, 9, 11, the changes to the maximum scour depth from $0.03 t_e$ to $0.25 t_e$ at three bed levels were 43%, 26% and 15%, respectively.

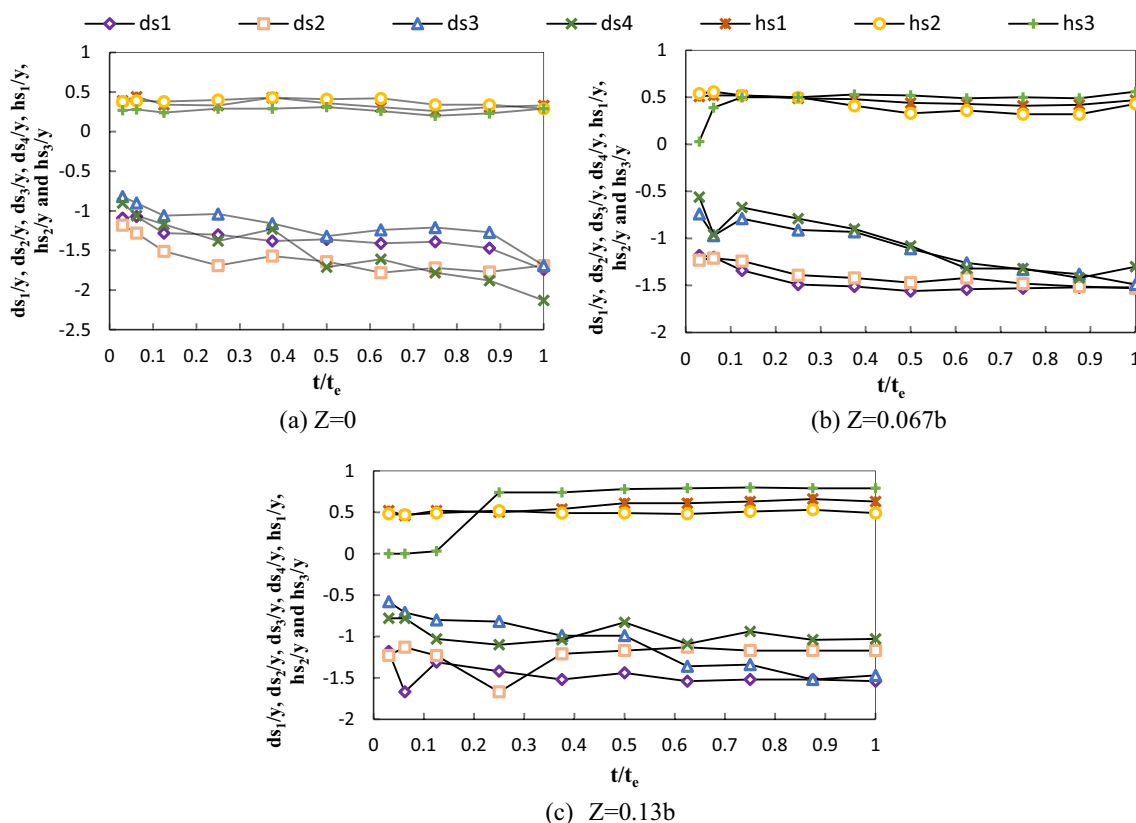


Fig. 13 Dimensionless temporal evaluations related to significant points

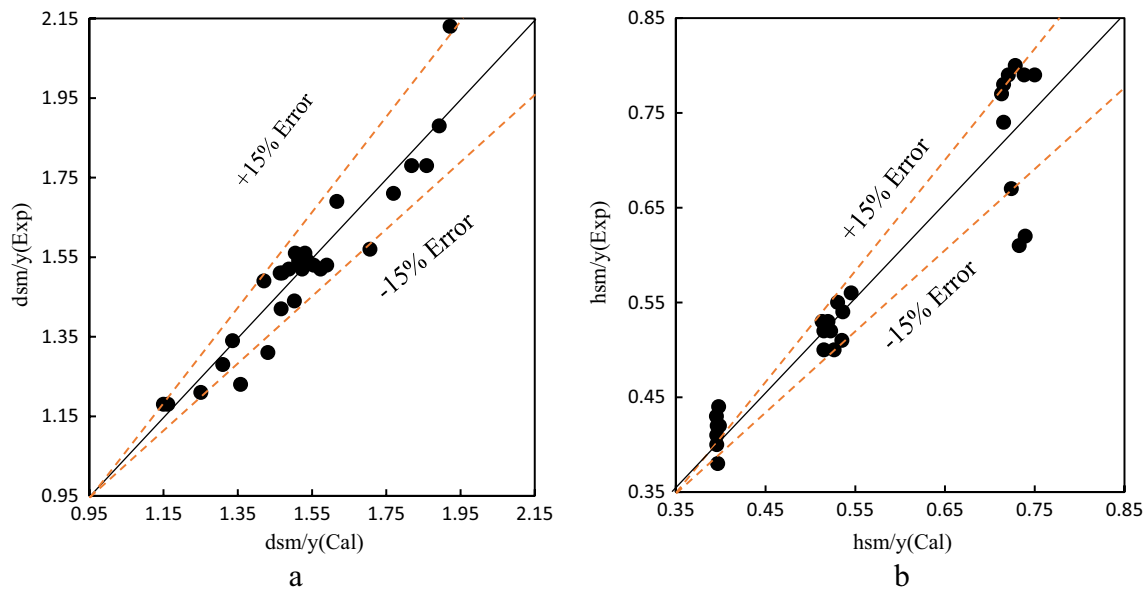


Fig. 14 Comparison of computational and observational values of **a)** the maximum scour and **b)** the maximum sedimentation

However, the changes to the maximum scour depth in $0.375 t_e$ to t_e at these three bed levels were 37%, 1.4% and 1.4%, respectively. This issue shows that by increasing the time of the experiment and approaching the equilibrium time, maximum scour depth variation decreased, which is in agreement with the Ghasemi and Ghodsian (2022) research (Ghasemi and Ghodsian 2022).

Table 2 illustrates the maximum scour depth values of three levels with their locations. This table shows the maximum scour depth in different experiment periods at the three levels with their locations. The values in the table have been made dimensionless with respect to the depth of water entering the culvert at each level. Water depth at the culvert inlet at levels $Z=0$, $Z=0.067b$ and $Z=0.13b$ was 0.09 m, and is indicated by y .

In Table 3, the maximum sedimentation values at the three levels are given along with their locations. In this table, as in Table 2, the values have been made dimensionless with respect to the depth of water entering the culvert. An important point illustrated by this table is that by increasing the experiment time and approaching the equilibrium time, maximum sedimentation occurred at a further distance from the culvert.

Figure 12 demonstrates the temporal evaluations of the maximum scour depth at the three levels. As shown in Fig. 12, the slopes of the maximum scour depth changes at levels $Z=0$, $Z=0.067b$ and $Z=0.13b$ were 0.95, 0.35 and 0.31, respectively, which reveals that the maximum slope change was related to level $Z=0$ and the minimum slope change occurred at level $Z=0.13b$. Also, it can be seen that, at the beginning of the experiment, the slope

Table 5 Quantitative values of the statistical parameters

| Bed level | Parameter | ds_m/y | hs_m/y |
|-------------|-----------|----------|----------|
| $Z=0.0b$ | RMSE | 0.090765 | 0.04013 |
| | MAE | 0.071261 | 0.0343 |
| | MSE | 0.008238 | 0.00161 |
| | MAPE | 4.17331 | 8.621562 |
| $Z=0.067b$ | RMSE | 0.042993 | 0.01612 |
| | MAE | 0.037186 | 0.013937 |
| | MSE | 0.001848 | 0.00026 |
| | MAPE | 2.554717 | 2.645147 |
| $Z = 0.13b$ | RMSE | 0.107346 | 0.073812 |
| | MAE | 0.072549 | 0.067498 |
| | MSE | 0.011523 | 0.005448 |
| | MAPE | 5.103768 | 9.260359 |

changes at all three levels were high, but they decreased with increase in the experiment time.

Figure 13 illustrates the temporal evaluations of the maximum scour depth and maximum sedimentation related to the selected zones in Fig. 5.

Figure 13a reveals that the lowest amount of scouring in all experiment time periods occurred in zone ds_3 . At this level, scouring increased with time in zone ds_4 and reached the highest value of all scouring zones in experiment with time t_e . Also, because of the surface vortexes near the channel bank at this level, sedimentation increased on the sides of the channel, and, as is clear, in 90% of the experiments, the lowest amount of sedimentation occurred in zone hs_3 .

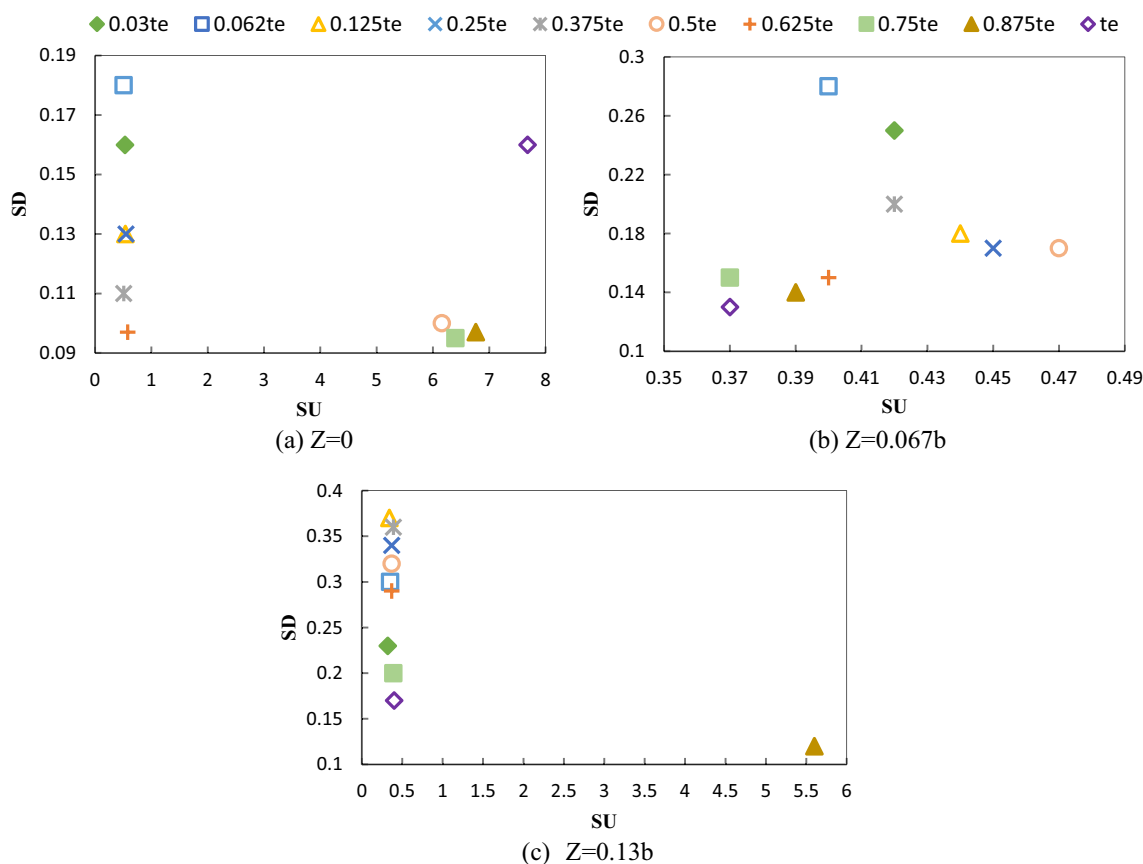


Fig. 15 Temporal evaluations of upstream and downstream slopes of scour holes

As Fig. 13b reveals, in 80% of the experiments, the maximum amount of scouring occurred in ds_1 , and the lowest scouring rate was observed in ds_4 . At this level, in hs_3 , sedimentation changed from minimum to maximum by increasing the experiment time in all zones. In experiment with $0.03 t_e$, sedimentation did not move forward into hs_3 , where sedimentation was zero.

Figure 13c shows that maximum scour depth in 80% of the experiments as $Z=0.067b$ appeared in zone ds_1 . Also at this level, in time $0.03 t_e$, scouring was lowest, and, by increasing the experiment time up to $0.875 t_e$, scouring reached maximum and occurred near ds_1 , and, in the equilibrium time, it occurred near ds_1 with a slightly different value. At this level, it can be seen that the sedimentation in the experiments with $0.03 t_e$, $0.062 t_e$ and $0.125 t_e$ in hs_3 was a negative value. In the other words, at this zone, instead of sedimentation, scouring appeared. This was due to the fact that with bed reductions, at first, the scour hole was quickly formed downstream of the culvert and, then, as more water flowed into the hole, the erosive power of the flow decreased, and the hole which was filled with water functioned as a damper for the falling jet.

Under totally similar conditions in terms of flow characteristics (the discharge, the Froude number, and the ratio of flow velocity to critical velocity) as well as the culvert and the channel's geometry, Sadeghpour et al. (2023) found that the highest amount of scouring occurred when the height, the roughness length and the distance between the installed roughness rows were respectively 5, 5 and 12 cm. The scour under this condition was equal to 20.1 cm. However, in this study, where no artificial roughness was installed, the highest amount of scouring occurred at the level of $Z=0$ for a duration equal to the equilibrium time, resulting in a scouring amount of 19.2 cm. Hence, this study shows a 4.5% difference in the maximum scour compared to that of Sadeghpour et al. (2023).

Equations 1 and 2 are presented for the sake of computing the values of the maximum scour and the maximum sedimentation. Table 4 shows the coefficients of these equations.

$$\frac{ds_m}{y} = a + b \ln\left(\frac{t}{t_e}\right) \tag{1}$$

$$\frac{hs_m}{y} = a + b \left(\frac{t}{t_e}\right) \ln\left(\frac{t}{t_e}\right) \tag{2}$$

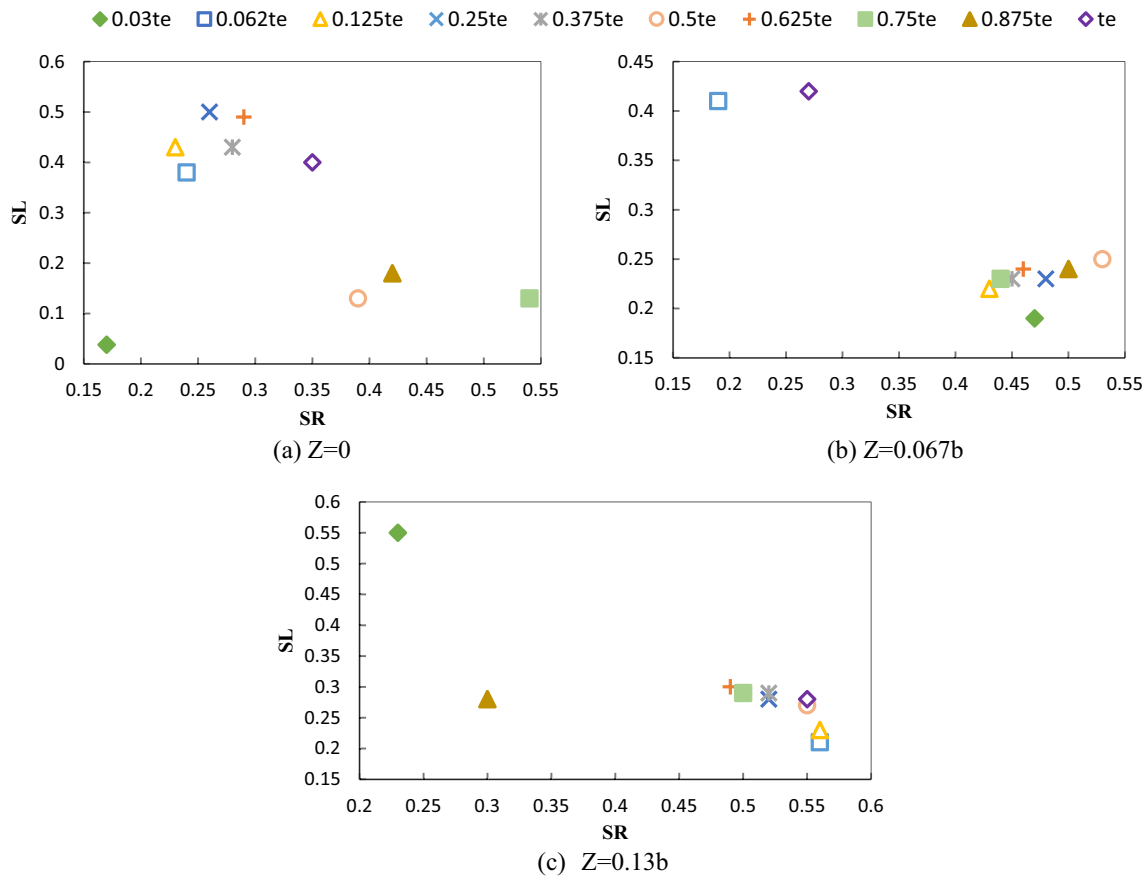


Fig. 16 Temporal evaluations of the slope of scour holes towards the right and left walls

Figure 14 compares the dimensionless computational and observational values of the maximum scour and sedimentation.

In addition, the following relations are presented for computing the quantity difference between the maximum scour and sedimentation values of the experiments and the computations (Safaripour et al. 2020; Vaghefi et al. 2023). \emptyset in these relations denotes the maximum scour depth or the maximum sedimentation. Figure 17 presents the cross sections of the three different bed levels. This section was located at point 0.12Y of the downstream of the culvert. These sections had changes in the shape of W and indicated twin scour holes located in about 80% of the middle of the channel.

$$RMSE = \sqrt{\frac{\sum_{i=1}^N (\emptyset_i^{cal} - \emptyset_i^{exp})^2}{N}} \tag{3}$$

$$MAE = \frac{\sum_{i=1}^N |\emptyset_i^{cal} - \emptyset_i^{exp}|}{N} \tag{4}$$

$$MSE = \frac{1}{N} \sum_{i=1}^N (\emptyset_i^{cal} - \emptyset_i^{exp})^2 \tag{5}$$

$$MAPE = \frac{100}{N} \sum_{i=1}^N \frac{|\emptyset_i^{cal} - \emptyset_i^{exp}|}{|\emptyset_i^{cal}|} \tag{6}$$

Table 5 presents the quantitative values for computing the statistical parameters for the sake of accuracy of the values obtained from the above relations relative to the experimental values.

Figure 15 illustrates the slopes of the scour holes upstream and downstream at all three levels and in different experiment periods. To calculate the slope of the hole, the maximum scour depth in the hole was considered, its cross section was determined, and the points which formed the highest part of the hole in the longitudinal direction upstream and downstream were taken into consideration. The ratio of the difference between the height of these points and maximum scour depth to the difference between their distances from each other provided the slope of the holes.

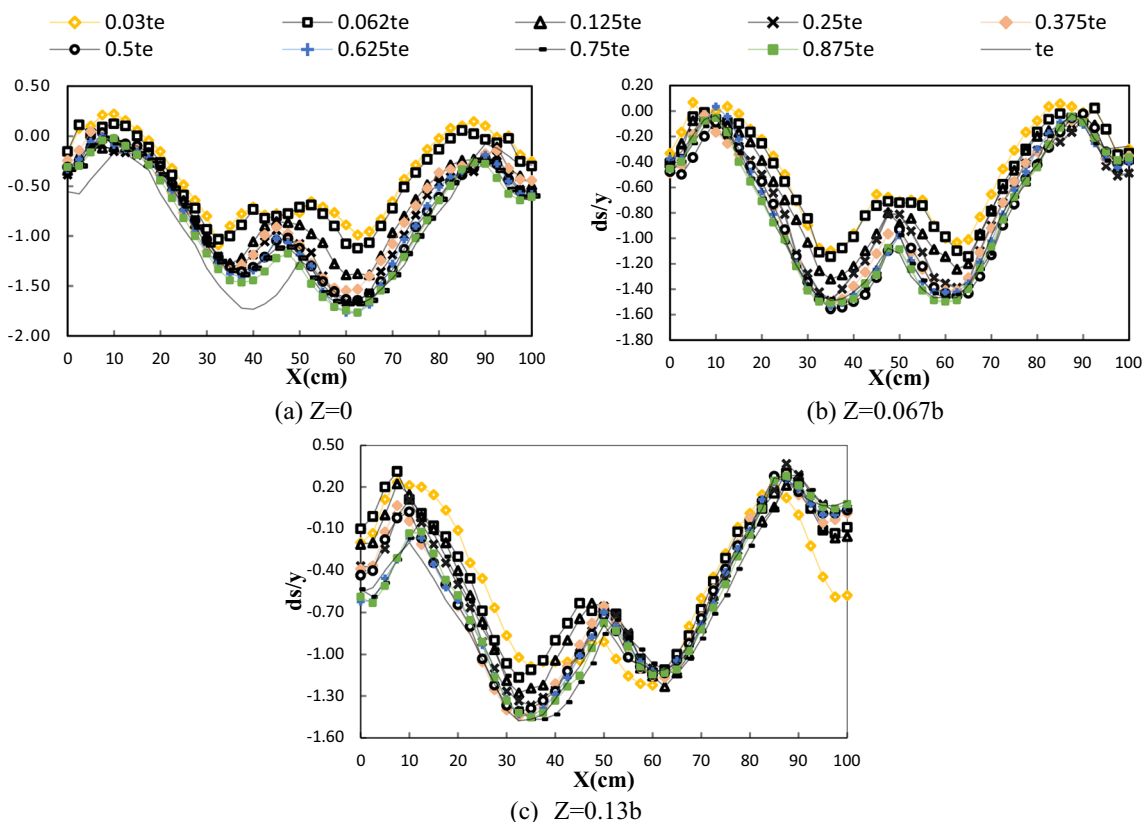


Fig. 17 Transverse profile at a distance of $0.12Y$ downstream of the culvert

Figure 15a shows that in experiments with $0.5 t_e$, $0.75 t_e$, $0.875 t_e$ and t_e , the hole slope in upstream was very high. According to Fig. 7 and Table 2, in these four experiments, the maximum scour holes occurred in holes that were close to the culvert. As a result, the slopes of these holes increased toward the culvert which was located upstream.

As shown in Fig. 15b, by increasing the time of the experiment, the slope of the holes gradually decreased toward the downstream. In this figure, the lowest slope of hole both toward upstream (SU) and downstream (SD) belong to the experiment with t_e . The hole related to the above-mentioned experiment had a large area because of its low slope, and its size was about 56% of the downstream length of the culvert.

Figure 15c reveals that the slope of the hole in experiment with $0.875 t_e$ toward upstream was higher than those of the other experiments. According to Fig. 11 and Table 2, the maximum scouring in this experiment occurred in a hole close to the culvert and had a high slope toward the culvert (i.e., upstream of the hole). In the rest of the experiments, at this level, the hole was located at a further distance from the culvert, which caused those slopes to be milder.

Figure 16 demonstrates the slopes of the holes toward the right and left walls of the channel at three different bed levels. To calculate the slope of a hole, the maximum scour depth in the hole was considered and its longitudinal section

was determined. Then, in the direction of the cross-section and toward the right and left walls of the channel, the highest point of the hole was determined and by calculating the ratio of the difference between the height of these points and the maximum scour depth to their distances from each other, the slope of the hole was obtained.

In Fig. 16a, it can be seen that the lowest slope of the hole toward the left and right walls of the channel occurred in the experiment with $0.03 t_e$. This shows that the hole in this experiment was broad with a width of about 90% of the channel width.

Figure 16b reveals that in two experiments with $0.062 t_e$ and t_e , the slope of the hole toward the left wall (SL) was higher, while, in the rest of the experiments, the slope of the hole toward the right wall (SR) was higher. According to Table 2, the maximum scour depth in the two above-mentioned experiments appeared in the hole near the left wall (ds_2), while, in the rest of the experiments, the maximum scour hole was near the right wall (ds_1). As a result, with the maximum scour depth appearing in the holes near the walls of the channel, the slope of the hole increased relative to the wall.

Figure 16c shows that the slope of the hole in $0.03 t_e$ reached the maximum level, relative to the left wall. This is unlike the other two levels at which a lower hole slope

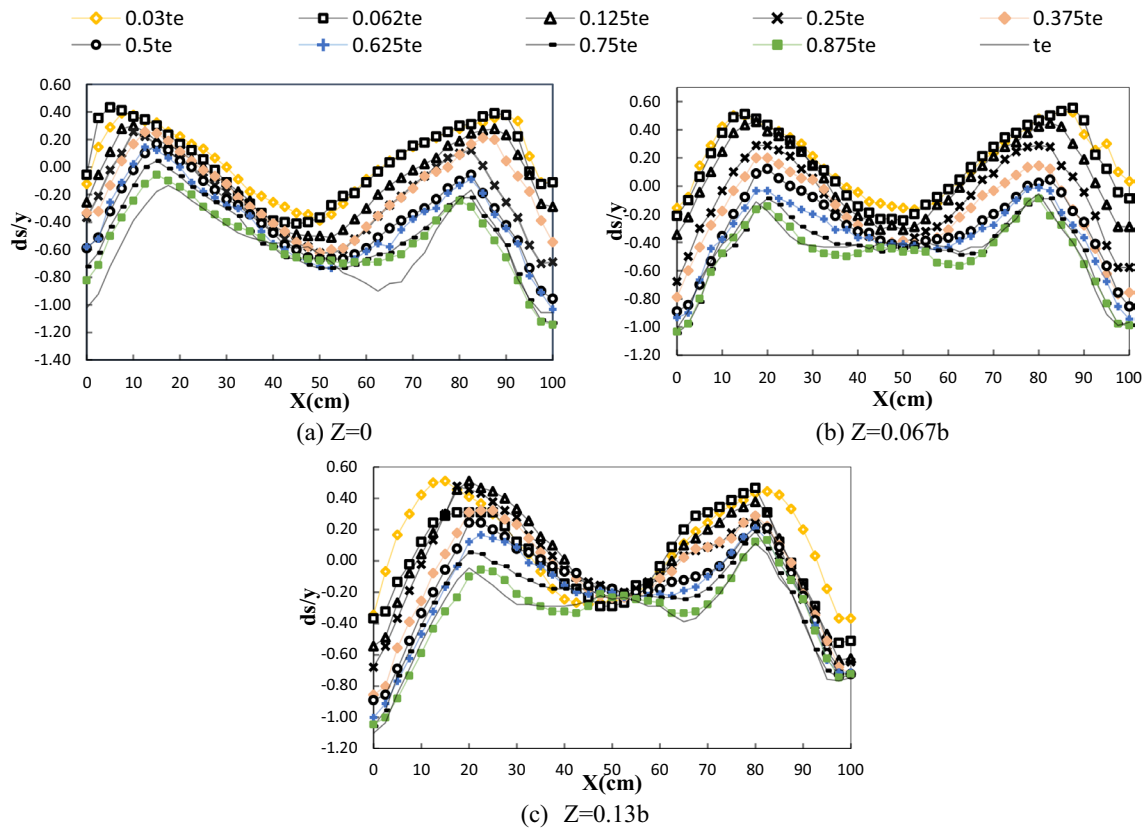


Fig. 18 Transverse profile at a distance of 0.32Y downstream of culvert

occurred in this experiment time, compared to the left wall.

Figure 17 presents the cross sections of the three different bed levels. This section was located at point 0.12Y of the downstream of the culvert. These sections had changes in the shape of W and indicated twin scour holes located in about 80% of the middle of the channel.

Figure 18 illustrates the cross sections at a distance of 0.32Y from downstream of the culvert at three different bed levels. In this figure, the changes of the sections from W, presented in Fig. 16, to M indicate the unification of the twin holes in the previous part and reduction of the amount of scouring, compared to the previous conditions, by moving towards the downstream.

Figure 19 shows the cross sections of the three bed levels at a distance of 0.72Y from downstream of the culvert. At these sections, the change in the bed form is completely evident, compared to the upstream sections. In the middle of these sections, change from scouring to sedimentation, and, near the banks, change from sedimentation to scouring are evident.

In Fig. 19c, it can be seen that the two experiments with $0.03 t_e$ and $0.062 t_e$ showed different behavior at this level, compared to other experiments. This can be explained by the

fact that, as seen in Fig. 11, due to the short time of these experiments, the sedimentation did not reach this section at a distance of 0.72Y, but scouring was observed there.

The transverse profile up to a distance of 0.12Y is shaped like a W and this profile shape literally indicates relatively stable culvert outlet banks, which prevent water movement toward the sides and floodplains. Then, when the profile shape changes from W into M in Figs. 17, 18, observed at distances of 0.32Y and 0.72Y, the sediments prevent the flow movement on the main path and therefore the flow is directed to the sides, which literally indicates the flow transport toward the surrounding floodplains.

Figure 20 shows the longitudinal profiles of the three bed levels at a distance of 0.4X from the right bank. According to Fig. 20a, the depth of scour holes in experiments with time t_e was considerably different from those in the other experiments. As the figure shows, from a distance of about 3–4 times the width of the culvert to its downstream, the bed profile changed from scouring to sedimentation. Of course, by changing the bed level and further decrease in downstream, the bed topography changed back to scouring. The process of this change was evident at level $Z = 0.13b$.

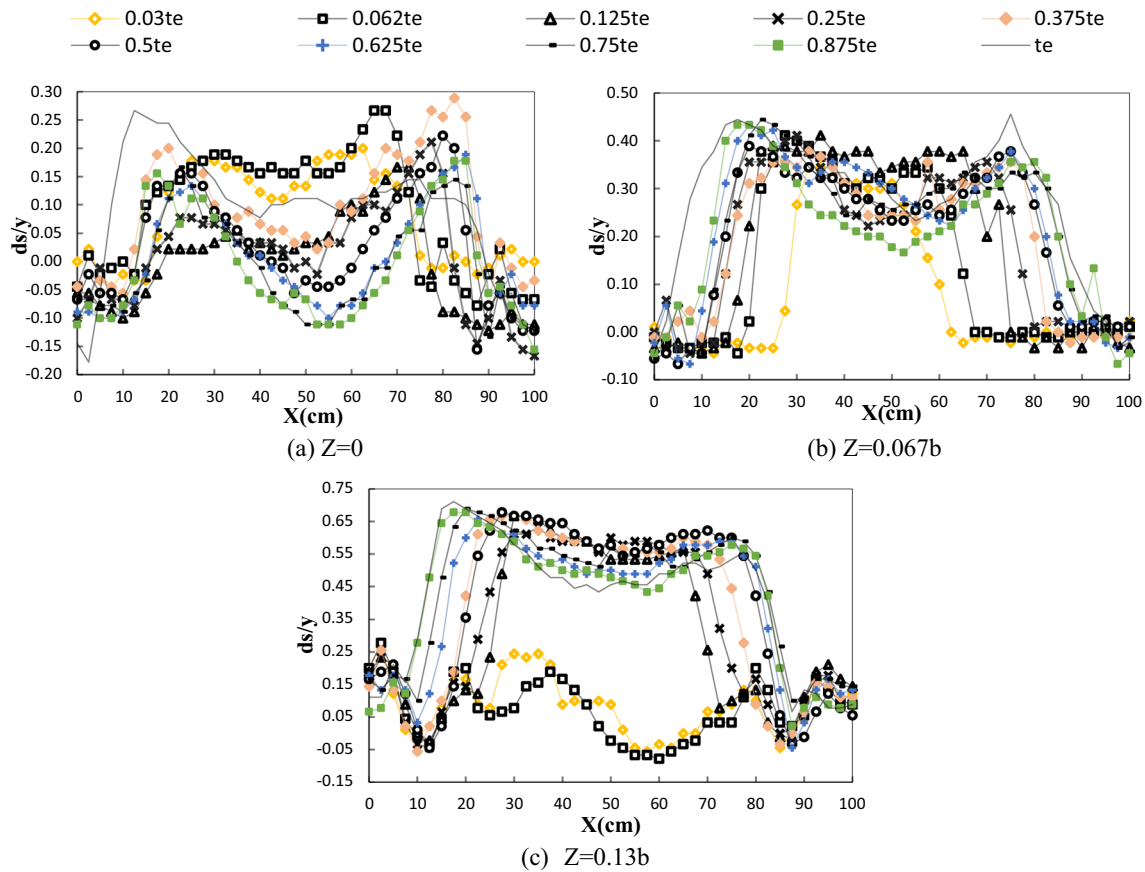


Fig. 19 Transverse profile at a distance of $0.72Y$ downstream of culvert

Figure 21 illustrates the longitudinal profiles at three different levels at a distance of $0.6X$ from the right bank. As can be seen, the dominant pattern in the bed form changes with scouring-sedimentation. By changing the bed level and further reduction in it, the pattern tended to be scouring-sedimentation-scouring, as shown in Fig. 20.

Figure 20a shows that the longitudinal profile was scoured in all experiment time periods up to a distance of $0.5Y$, and, after that, sedimentation started. However, according to Fig. 21a, the bed profile was located in the scouring zone up to a distance of $0.35Y$. Also, as seen in Fig. 20b, the bed profile was located in the scouring zone up to a distance $0.6Y$ while, according to Fig. 21b, the bed profile at a distance of less than $0.5Y$ was in the form scouring, and, after that, sedimentation occurred. In Figs. 20c and 21c, the bed profile appears in the scouring zone in both situations up to a distance of about $0.8Y$.

Figure 22 illustrates the area and volume of total scouring at three different bed levels in different experiments, with values made dimensionless with respect to depth. This figure shows that, by decreasing the bed level, the volume of scouring increased. Also, by increasing the time of the experiment at level $Z=0$, the volume and area of

total scouring decreased. In $0.375 t_e$, however, according to Fig. 7, scour holes turned deeper, compared to other test periods, and, in t_e , the maximum amount of scouring considerably increased. In these two test periods only, the volume and area of scouring increased.

At level $Z=0$, the maximum volume and area of scouring appeared in experiment with $0.062 t_e$ while the lowest volume and area of scouring occurred in experiment with $0.875 t_e$.

As shown in Fig. 22c, by increasing the experiment time, the total volume of scouring increased. Figure 22d compares the area and volume of scouring at the three levels in all experiments. It can be seen that, in 90% of the experiments, the area of scouring was greater than the volume of scouring hole quantitatively.

Figure 23 illustrates the area and volume of sedimentation in different experiments, with values made dimensionless by depth. This figure indicates that by increasing the experiment time, the total volume of sedimentation increased. At level $Z=0$, by increasing the time of the experiment, the area of sedimentation increased. But, by decreasing the bed level, as with level $Z=0.13b$, over time and with increasing the time of the experiment, the area of sedimentation decreased.

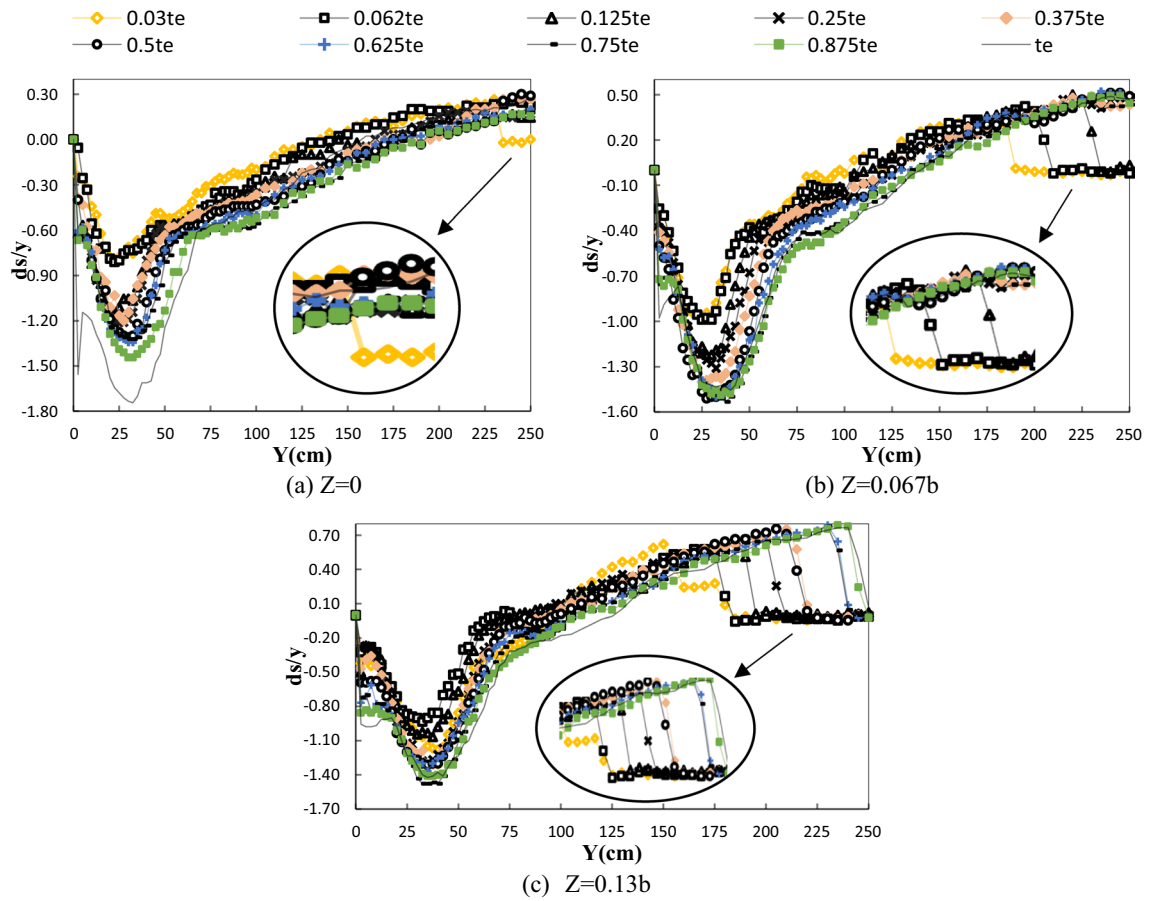


Fig. 20 Longitudinal profile at a distance of $0.4X$ from the right wall of the channel

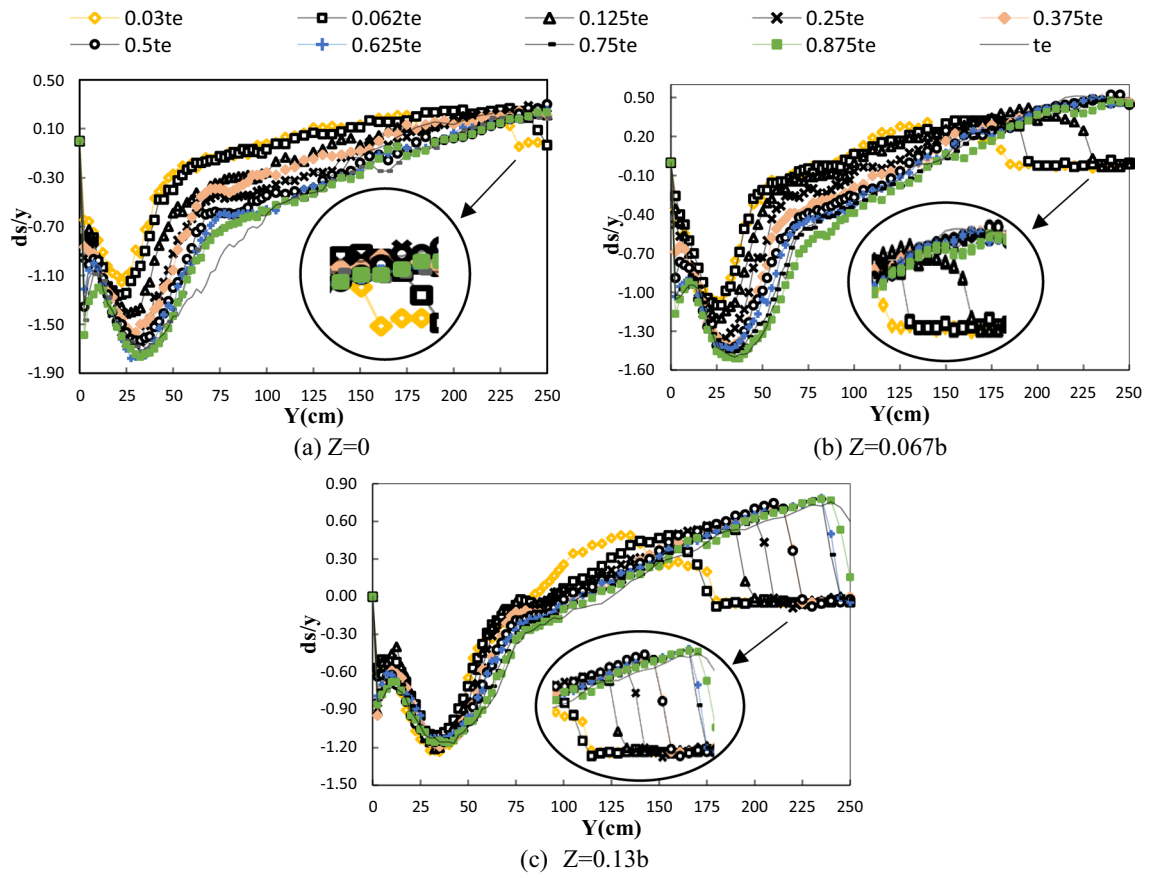


Fig. 21 Longitudinal profile at a distance of $0.6X$ from the right wall of channel

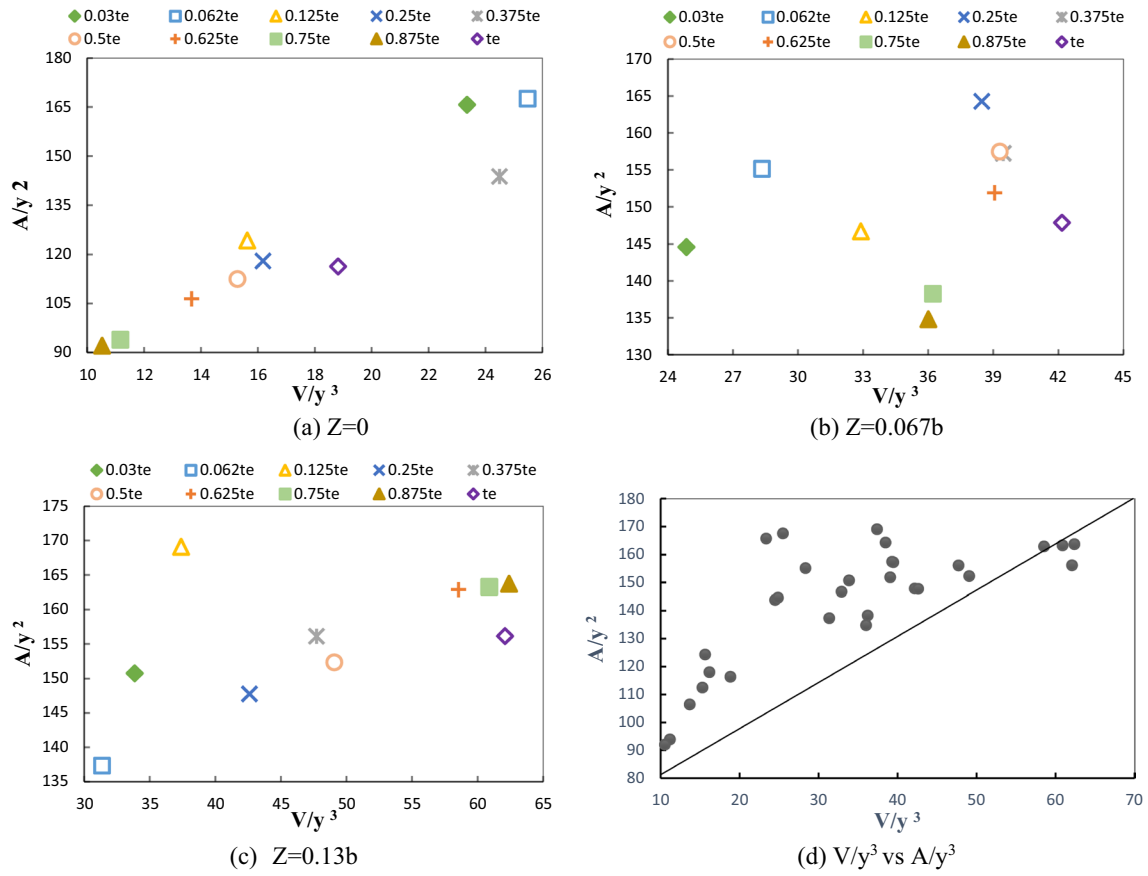


Fig. 22 Temporal evaluations of area and volume of total scouring

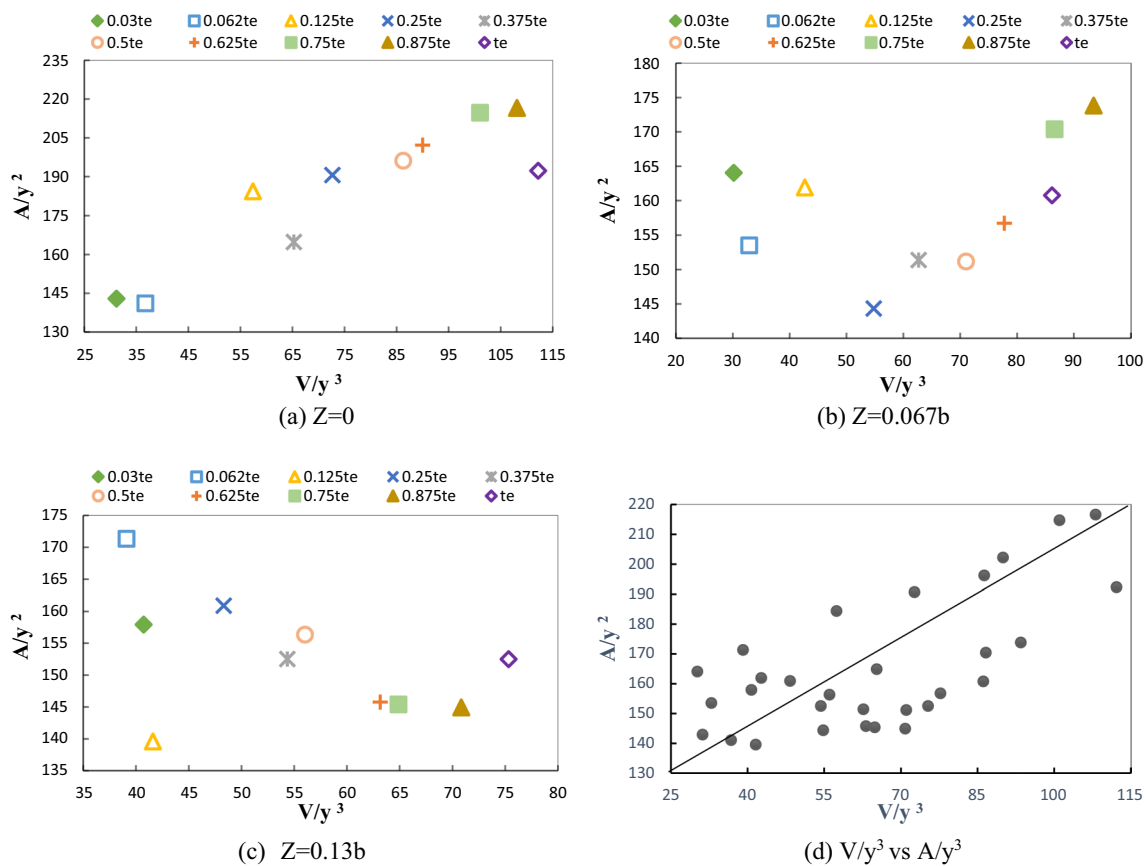


Fig. 23 Temporal evaluations of the area and total volume of sedimentation

Figure 23d represents the distribution of points in the first and third quadrants regarding the dimensionless area and volume of the sedimentation.

Conclusion

In this research, the temporal evaluations of bed topography downstream of a rectangular culvert at different levels were investigated.

The following results were obtained:

1. By decreasing the bed level downstream of a culvert, the rate of sediment movement towards the downstream of the culvert decreased.
2. By approaching the equilibrium time, the percentage of changes to the maximum scouring depth decreased.
3. The slope of the variation of maximum scour depth at $Z=0.067b$ and $Z=0.13b$ showed no significant changes, compared to level $Z=0$.
4. The amount of maximum scour depth at level $Z=0$ in experiment with time $0.125 t_e$ was equal to 98% of maxi-

imum scour depth in experiment t_e at levels $Z=0.067b$ and $Z=0.13b$.

5. The slope of scour holes with respect to the channel walls, close to which the maximum scour depth appeared, was higher than the slope of scour holes toward the other wall.
6. By decreasing the bed level, the total volume of scouring increased.
7. The dimensionless area of scour holes in 90% of the experiments was greater, compared to the dimensionless volumes of scouring holes, which showed the expansion of the scour holes.

Author contributions The authors declare that they have contribution in the preparation of this manuscript. All authors read and approved the final manuscript.

Funding The authors received no funding for this work.

Availability of data and materials All data generated or analyzed during this study are included in this published article.

Declarations

Conflict of interest The authors have no relevant financial or non-financial interests to disclose.

Ethical approval This work has not been published elsewhere nor is it currently under consideration for publication elsewhere.

Consent for publication The authors agree to publish this manuscript upon acceptance.

Consent to participate The authors have read the final manuscript, have approved the submission to the journal and have accepted full responsibilities pertaining to the manuscript's delivery and contents.

Open Access This article is licensed under a Creative Commons Attribution 4.0 International License, which permits use, sharing, adaptation, distribution and reproduction in any medium or format, as long as you give appropriate credit to the original author(s) and the source, provide a link to the Creative Commons licence, and indicate if changes were made. The images or other third party material in this article are included in the article's Creative Commons licence, unless indicated otherwise in a credit line to the material. If material is not included in the article's Creative Commons licence and your intended use is not permitted by statutory regulation or exceeds the permitted use, you will need to obtain permission directly from the copyright holder. To view a copy of this licence, visit <http://creativecommons.org/licenses/by/4.0/>.

References

- Abt SR, Ruff JF, Doehring FK, Donnell CA (1985) Culvert slope effect on outlet scour. *J Hydraul Eng* 111(10):1363. [https://doi.org/10.1061/\(ASCE\)0733-9429\(1985\)111:10\(1363\)](https://doi.org/10.1061/(ASCE)0733-9429(1985)111:10(1363))
- Abt SR, Ruff JF, Doehring FK, Donnell CA (1987) Influence of culvert shape on outlet scour. *J Hydraul Eng* 113(3):393. [https://doi.org/10.1061/\(ASCE\)0733-9429\(1987\)113:3\(393\)](https://doi.org/10.1061/(ASCE)0733-9429(1987)113:3(393))
- Ahmed KO, Amini A, Bahrami J, Kavianpour MR, Hawez DM (2021) Numerical modeling of depth and location of scour at culvert outlets under unsteady flow conditions. *J Pipeline Syst Eng Pract.* [https://doi.org/10.1061/\(ASCE\)PS.1949-1204.0000578](https://doi.org/10.1061/(ASCE)PS.1949-1204.0000578)
- Aksoy AO, Dogan M (2019) Experimental investigation of time-dependent local scour downstream of a stepped channel. *Water SA.* <https://doi.org/10.17159/wsa/2019.v45.i3.6738>
- Aminpour Y, Farhoudi J, KhaliliShayan H, Roshan R (2018) Characteristics and time scale of local scour downstream stepped spillways. *Sci Iran* 25(2):532–542. <https://doi.org/10.24200/sci.2017.4187>
- Ben Mohammad Khajeh S, Vaghefi M (2020) Investigation of abutment effect on scouring around inclined pier at a bend. *J Appl Water Eng Res* 8(2):125–138. <https://doi.org/10.1080/23249676.2020.1761898>
- Dodaro G, Tafarojnoruz A, Calomino F, Gaudio R, Stefanucci F, Adduce C, Sciortino G (2014) An experimental and numerical study on the spatial and temporal evolution of a scour hole downstream of rigid bed. Taylor and francis group, London, ISBN 978-1-138-02674-2. <https://doi.org/10.1201/b17133-189>
- Doehring K, Abt SR (1994) Drop height influence on outlet scour. *J Hydraul Eng* 120(12):1470. [https://doi.org/10.1061/\(ASCE\)0733-9429\(1994\)120:12\(1470\)](https://doi.org/10.1061/(ASCE)0733-9429(1994)120:12(1470))
- Eghbali L, Vaghefi M, Golbaharhaghghi MR (2019) Laboratory study of the temporal evolution of channel bed topography in presence of two rows of inclined-vertical piers in a sharp 180-degree bend. *ISH J Hydraul Eng.* <https://doi.org/10.1080/09715010.2019.1674700>
- Emami S, Shciels A (2010) Prediction of localized scour hole on natural mobile bed at culvert outlet. In: Proceeding 5th international conference on scour and erosion(ISCE-5). San Francisco, Usa. Reston, Va.: American society of civil engineers. S. pp 844–853. [https://doi.org/10.1061/41147\(392\)84](https://doi.org/10.1061/41147(392)84)
- Galan A, Gonzalez J (2019) Effects of shape, inlet blockage and wing walls on local scour at the outlet of non-submerged culverts: undermining of the embankment. *Environ Earth Sci* 79(25):1–16. <https://doi.org/10.1007/s12665-019-8749-3>
- Ghasemi E, Ghodsian M (2022) Scouring downstream of sediment-carrying free over fall water jet. *Iran Hydraul Assoc.* <https://doi.org/10.30482/jhyd.2021.285817.1529>
- Gunal M, Gunal AY, Osman K (2019) Simulation of blockage effects on scouring downstream of box culverts under unsteady flow conditions. *Int J Environ Sci Technol* 16:5305–5310. <https://doi.org/10.1007/s13762-019-02461-w>
- Horst M (2019) Influence of wingwall configuration on outlet scour at bottomless box culverts. *Int J Hydraul Eng* 8(1):7–10. <https://doi.org/10.5923/j.ijhe.20190801.02>
- Melville BW, Chiew YM (1999) Time scale for local scour at bridge piers. *J Hydraul Eng.* [https://doi.org/10.1061/\(ASCE\)0733-9429\(1999\)125:1\(59\)](https://doi.org/10.1061/(ASCE)0733-9429(1999)125:1(59))
- Mia MF, Nago H (2003) Design method of time-dependent local scour at circular bridge pier. *J Hydraul.* [https://doi.org/10.1061/\(ASCE\)0733-9429\(2003\)129:6\(420\)](https://doi.org/10.1061/(ASCE)0733-9429(2003)129:6(420))
- Moghaddassi N, Musavi-Jahromi SH, Khosrojerdi A (2021) Effect of duration on variations in bed topography and water surface profile in a meandering channel. *J Hydraul Struct.* <https://doi.org/10.22055/JHS.2021.37497.1173>
- Nasreen T, El-feky MM, El-saiad AA, Fathi S (2020a) Numerical investigation of scour characteristics downstream of blocked culverts. *Alex Eng J* 59:3503–3513. <https://doi.org/10.1016/j.aej.2020.05.032>
- Nasreen T, El-feky MM, El-saiad AA, Zelenakova M, Vranay F, Fathi S (2020b) Study of scour characteristics downstream of partially-blocked circular culverts. *Water* 12(10):2845. <https://doi.org/10.3390/w12102845>
- Oliveto G, Hager WH (2005) Further results to time-dependent local scour at bridge elements. *J Hydraul Eng* 131(2):97. [https://doi.org/10.1061/\(ASCE\)0733-9429\(2005\)131:2\(97\)](https://doi.org/10.1061/(ASCE)0733-9429(2005)131:2(97))
- Pandey M, Valyrakis M, Qi M, Sharma A, Lodhi AS (2021) Experimental assessment and prediction of temporal scour depth around a spur dike. *Int J Sediment Res.* 36(1):17–28. <https://doi.org/10.1016/j.ijsrc.2020.03.015>
- Sadeghpour M, Vaghefi M, Meraji SM (2023) Artificial roughness dimensions and their influence on bed topography variations downstream of a culvert: an experimental study. *Water Resour Manage.* <https://doi.org/10.1007/s11269-023-03543-8>
- Safaripour N, Vaghefi M, Mahmoudi A (2020) Experimental study of the effect of submergence ratio of double submerged vanes on topography alterations and temporal evaluation of the maximum scour in a 180-degree bend with bridge pier group. *Int J River Basin Manag.* <https://doi.org/10.1080/15715124.2020.1837144>
- Solati S, Vaghefi M (2020) Behrooz AM (2020) Effect of duration and pattern of hydrographs on scour around pier in sharp bend under incipient motion and live bed conditions. *Int J Civil Eng* 19:51–65. <https://doi.org/10.1007/s40999-020-00558-9>
- Sorourian S, Keshavarzi A, Ball J, Samali B (2013) Study of blockage effect on scouring pattern downstream of a box culvert under unsteady flow. *Aust J Water Resour* 18(2):180–190. <https://doi.org/10.7158/W13-031.2014.18.2>
- Sung-Uk C, Byungwoong C (2016) Prediction of time-dependent local scour around bridge piers. *Water Environ J.* <https://doi.org/10.1111/wej.12157>

- Vaghefi M, Ghodsian M, SalehiNeysaboori SAA (2009) Experimental study on the effect of T-shaped spur dike length on scour in a 90 channel bend. *Arab J Sci Eng* 34:337
- Vaghefi M, Zarei E, Ahmadi G, Behrozi AM (2023) Experimental analysis of submerged vanes' configuration for mitigating local scour at piers in a sharp bend: influence of quantity, length, and orientation. *Ocean Eng*. <https://doi.org/10.1016/j.oceaneng.2023.116267>
- Yanmaz AM, Altinbilek HD (1991) Study of time-dependent local scour around bridge piers. *J Hydraul Eng* 117(10):1991. [https://doi.org/10.1061/\(ASCE\)0733-9429\(1991\)117:10\(1247\)](https://doi.org/10.1061/(ASCE)0733-9429(1991)117:10(1247))
- Yanmaz AM, Kose O (2007) Time-wise variation of scouring at bridge abutments. *Sadhana* 32:199–213. <https://doi.org/10.1007/s12046-007-0018-6>
- Zhang R, Peng W (2019) The investigation of shape factors in determining scour depth at culvert outlets. *ISH J Hydraul Eng*. <https://doi.org/10.1080/09715010.2019.1611492>

Publisher's Note Springer Nature remains neutral with regard to jurisdictional claims in published maps and institutional affiliations.